ELSEVIER

International Conference on Computational Science, ICCS 2011

Tungsten imido-catalysed dimerisation of α-olefins: insight into the Lewis acid's function revealed from computational studies

Sven Tobisch[a],*

[a]Sasol Technology (U.K.) Ltd, Purdie Building, North Haugh, St Andrews, UK KY16 9ST

Abstract

Alternative channels of the tungsten imido-catalysed olefin dimerisation proceeding through mono(imido) and bis(imido) compounds have been examined by means of the DFT method simulating authentic reaction conditions on catalyst models that closely mimic the real catalyst system. All relevant steps of a plausible metallacycle mechanism to follow alternative pathways together with the divergent path towards azatungstanacycle intermediates have been characterised by considering up to three $AlClMe_2$ moieties explicitly. This study disclosed that the Lewis acid is actively engaged in the productive catalytic cycle, this in addition to its presumed role, among others, as alkylating and chloride ligand abstraction agent in the formation of the active catalyst species. The Lewis acid preferably forms four-membered chelates across tungsten–imido or tungsten–chlorine bonds featuring a μ-Al–Cl–W bridge. The formation of the five-membered tungstanacycle is found to be less affected by the cocatalyst, but it acts profoundly in modulating the energetics of its degradation into the dimer product. DFT predicts a smooth energy profile for the most accessible path via mono(imido) tungsten species, having the Lewis acid bridged across tungsten–chlorine bonds, which is in consonance with observed activity and selectivity. This type of Lewis acid association appears as being pivotal for an effective catalysis. The alternative channel to engage bis(imido) tungsten compounds features significantly more demanding kinetics for the dimer generating route, thereby rendering it as being almost impossible to be accessed. The present study constitutes evidence, based on reliable DFT calculations, that mono(imido) tungsten compounds complexed by the Lewis acid component is effectively triggering dimerisation, whilst bis(imido) tungsten species are unlikely to play a role in the productive cycle.

Keywords: dimerisation; tungsten; mechanism; density functional calculation

1. Introduction

The dimerisation of low number α-olefins by homogeneous catalysts is an attractive, direct route towards specific higher olefins and represents an area of commercial and also academic significance [1]. This process has seen substantial research efforts in recent years [2]. A variety of catalyst systems has been reported for dimerising olefins, most of which yield branched dimers [1, 2], but certain late transition metal-based catalysts display abilities for linear dimerisation [3-6]. On the other hand, applications of group 6 metals are rather limited [2, 7], although of

---

* Corresponding author. Tel.: +44-1334-460-130; fax: +44-1707-383653.
E-mail address: sven.tobisch@eu.sasol.com.

recent advances in the development of chromium systems capable of trimerising ethylene selectively to 1-hexene [8, 9] and exhibiting some selectivity towards the tetramer, 1-octene [10].

Tungsten imido compounds are one of the rare examples, which have recently been reported of being capable dimerising α-olefins [11]. Catalyst systems prepared by treating a tungsten source (WCl_6 as an example) with one or two molar equivalents of aniline, together with the required amount of base and chloroaluminium alkyl activator of the type $AlCl_nR_m$ (m+n=3), both exhibit high selectivity towards dimerisation [11]. Hence, mono(imido) and bis(imido) tungsten compounds can be envisaged as triggering dimerisation catalysis (Scheme 1). A huge excess of the cocatalyst is often used for various oligomerisation and polymerisation catalyst systems [1, 2], where the cocatalyst is thought to play several roles in the generation of the active catalysts including the alkylation of transition metal chloride precursors, alkyl ligand abstraction to afford cationic transition metal species and scavenging of impurities. In contrast, the title reaction requires a distinct amount of the cocatalyst (~15 molar equivalents) [11], thereby alluding to a specific function of the Lewis acid in the productive catalytic cycle. However, little is known about the identity of the catalytically active species, which has not been unravelled thus far.

Utilising DFT calculations as a powerful tool capable of aiding in a broader understanding, we have recently examined selected steps of the dimerisation course for mono(imido) and bis(imido) tungsten catalysts, the key findings of which were disclosed previously [12]. Herein we report further computational studies on structural and energetic aspects of key intermediates, discussing competing pathways and comparing the alternative dimerisation channels depicted in Scheme 1. This will lead us to demonstrate theoretically the impact of the Lewis acid on dimerisation catalysis, to provide evidence for the identity of the catalytically competent species and to assign the turnover-limiting step.
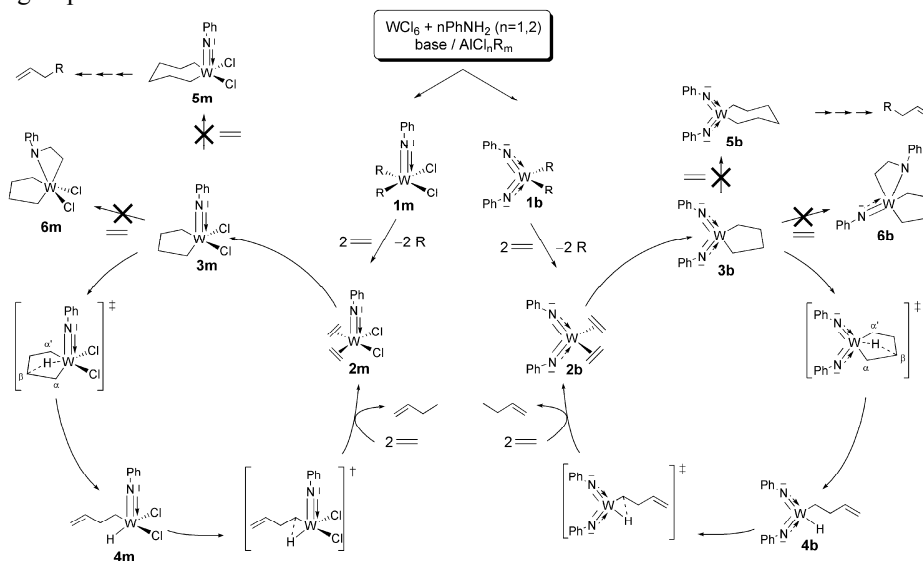
Scheme 1: Alternative channels for imido tungsten-catalysed olefin dimerisation, exemplified for prototypical ethylene.

2. Catalytic reaction course

Scheme 1 shows a plausible mechanistic scenario involving metallacycle intermediates, which have been unequivocally established for chromium-mediated ethylene oligomerisation and polymerization [13, 14]. Treatment of the WCl_6 starting material with one or two molar equivalents of aniline and the required amount of base gives initially rise to $[W(NPh)Cl_4]$ [15] and $[W(NPh)_2Cl_2]$ [16], which then leads presumably *in situ* to $[W(NPh)R_2Cl_2]$ (**1m**) and $[W(NPh)_2R_2]$ (**1b**) compounds, respectively, in the presence of the cocatalyst. The effective catalysis first entails conversion of **1m**, **1b** into the bis(olefin) species **2m**, **2b**, which represent the active catalyst species of the alternative dimerisation channels proceeding through mono(imido) and bis(imido) tungsten species. Oxidative

coupling of the olefin moieties generates the tungstana(IV)cyclopentane **3**. Its degradation to follow either the concerted 1,3-H transfer or a stepwise mechanism affords the dimer product. The latter has been found as being favourable for the conformationally rigid five-membered metallacycle intermediate [17] and comprises of consecutive β-H abstraction and reductive CH elimination with an intervening W–H–alkenyl intermediate **4**. Repeated olefin insertion into consecutively enlarged metallacycle fragments, to first yield the tungstana(IV)cycloheptane **5**, and subsequent degradation would lead to larger oligomers. Alternatively, olefin attack at the tungsten−imido linkage to form the azatungstanacycle **6** in a [2 + 2] cycloaddition would open a possible route that leads to catalyst deactivation.

3. Computational model and method

Model: Herein is reported the computational survey of alternative channels of the imido tungsten-mediated olefin dimerisation, with ethylene served as a prototypical α-olefin substrate. The catalyst model was chosen in such a fashion to closely mimic the real catalyst system [11]. This study employed $[W(NC_6H_5)Cl_2(C_2H_4)_2]$ and $[W(NC_6H_5)_2(C_2H_4)_2]$ to represent **1m**, **1b**, together with $AlClMe_2$ as Lewis acid component. We performed an extensive DFT simulation of configurationally and conformationally different reaction pathways involving up to three $AlClMe_2$ moieties, the most favourable of which are reported herein. Lewis acid association/dissociation and reorganisation have been probed for the various intermediates, but found to occur in an essentially barrierless fashion. This has been examined in a linear-transit approach, as the exact localisation of the TS structures is complicated by the flatness of the PES in these regions. Key species of the reaction course were denoted consistently with Arabic numbers as shown in Scheme 1, augmented by **m** or **b** characters to indicate mono(imido) and bis(imido) tungsten species, respectively.

Method: All DFT calculations were performed with the program package TURBOMOLE [18] using the TPSS density functional [19] in conjunction with flexible basis sets of triple-ζ quality. For W we used the Stuttgart−Dresden quasirelativistic effective core potential (SDD) with the associate (8s7p6d)/[6s5p3d] valence basis set [20]. All other elements were represented by Ahlrich's valence triple-ζ TZVP basis set [21] with polarization functions on all atoms. The good to excellent performance of the TPSS functional for a wide range of applications has been demonstrated previously [22].

All stationary points were located by utilizing analytical/numerical gradients/Hessians according to standard algorithms without imposing any symmetry constraints and were identified exactly by the curvature of the potential-energy surface at these points corresponding to the eigenvalues of the Hessian. The reaction and activation free energies (ΔG, $\Delta G^{\ddagger}$ at 298 K and 1 atm) were evaluated according to standard textbook procedures [23] using computed harmonic frequencies. The influence of the solvent (chlorobenzene) [11] was taken into explicit consideration by making use of a continuum model. All the key species were fully located with inclusion of solvation by the COSMO method [24]. In order to account for real condensed-phase reaction condition, the entropy costs for Lewis acid and olefin substrate association/dissociation processes was approximated as being two-thirds of its gas-phase value. This approximation was successfully applied in former investigations on group 4 metal-assisted selective olefin oligomerisation [17d, 25] and is expected to reasonably estimate the true entropy contribution in condensed phase.

4. Results and discussion

This study is divided into two parts. The first part aims at gauging computationally what influence the cocatalyst exerts on individual elementary steps. Important aspects already disclosed in previous communications [12] are summarised briefly, but will be extended by the exploration of alternative modes for Lewis acid association and of rival pathways. The most accessible routes of the alternative dimerisation channels will be compared in the second part.

4.1. Exploration of the cocatalyst's influence onto relevant elementary steps.

4.1.1. Thermodynamics of Lewis acid association

We start with the assessment of the strength of Lewis acid association onto the key intermediate of the dimerisation course, *viz*. tungstanacycle **3**. The analysis is confined to interactions of the cocatalyst with the immediate environment around the tungsten centre. Hence, up to three and two AlClMe$_2$ moieties, respectively, have been explicitly considered for **3m** and **3b**. Off the various tested association modes, a four-membered chelate featuring a μ-Al–Cl–W bridge revealed as being favourable. Two different motifs are seen in Fig. 1 for **3m**, where the Lewis acid bridges the tungsten–imido bond (type A) or exclusively the tungsten–chlorine bond (type B). The dianionic imido ligand acts as net six-electron donor to the electron-deficient tungsten centre in unbound **3m-0**, as it is evident from the near linear tungsten–imido linkage (∢W=N–R = 178°) [26]. Complexation at the chlorine centre weakens somewhat the equatorial W–Cl bond, which is near-balanced by new W→Cl and Al→Cl dative bonds, but leaving the tungsten–imido bond unaffected. Type B adducts are thus the preferred of the two association motifs, with **3m-IB** and **3m-IIB** are only moderately uphill (Fig. 1). This contrasts with type A adducts, where the generation of a N$_{imide}$→Al interaction provokes substantial electronic reorganisations at the nitrogen centre, effectively attenuating the tungsten–imido bond to a degree that cannot be compensated for by the newly formed dative bonds. As a result, **3m-IA**, **3m-IIA** and **3m-IIIA** are thermodynamically highly unfavourable (Fig. 1).

A different situation arises for uncomplexed **3b-0**, where the imido's lone pairs share the same vacant tungsten orbital. Hence, some proportion of the lone pair's density remains localised on each nitrogen atom, as manifested in two distinctly bent imido moieties (∢W=N–R = 161°) showing equally lengthened W=NR bonds (1.796 Å, Fig. 1). The higher basicity of N$_{imide}$ centres makes bis(imido) tungsten(VI) compounds more susceptible towards Lewis acid bridging across the arylimido–tungsten linkage than their mono(imido) cousins. Chelation of one of the imido groups greatly benefits from the second unbound imido group acting stabilising as a net six electron donor (∢W=N–R = 179°, 1.765 Å). Species **3b-I** has been predicted previously by us as the favourable and stable Lewis acid adduct of a bis(imido) tungsten(VI) compound (Fig. 1).

The four-membered chelates depicted in Fig. 1 are seldom reported in literature [27, 28]. One notable example is the X-ray structure of an AlMe$_3$ adduct of a titanium imido methyl cation featuring two bridged methyl groups [28]. Supportive DFT calculations by the same authors have indicated that steric factors govern the observed association mode, whilst bridging the titanium–imido bond is preferred electronically. Alternative forms of AlClMe$_2$ association onto **3m**, **3b** featuring a μ-Al–Me–W bridge have been probed explicitly, the relative stabilities, given in parenthesises, are collected in Fig. 1. This clearly shows the greater aptitude of the chlorine donor centre to participate in AlClMe$_2$ association.

Table 1: Calculated free-energy profile ($\Delta G^{\ddagger}$, ΔG in kcal mol^{-1})^a for **2** → **3** oxidative coupling proceeding through mono(imido) and bis(imido) tungsten compounds

association mode^b	TS[**2–3**]	**3**
mono(imido) **2m**		
0	7.0	−2.3
IA	13.6	1.7
IB	17.0	4.1
IIA	13.3	−1.3
IIB	16.3	3.9
IIIA	15.9	2.8
bis(imido) **2b**		
0	7.5	−1.6
I	6.3	1.1
II	10.9	−1.9

^{a} Intrinsic energetics relative to the respective precursor species **2m**, **2b**. ^{b} See Fig.1.

4.1.2. Formation of five-membered tungstanacycle intermediate 3

The first step in the productive cycle is the **2**→**3** oxidative coupling, the energetics of which is summarised in Table 1 for the various pathways. For unbound precursors **2m-0** and **2b-0**, this is a remarkable facile ($\Delta G^{\ddagger} < 8$ kcal

mol^{-1}) slightly exergonic process, thus proceeding in a reversible fashion. Olefin coupling remains mainly thermoneutral but becoming more demanding kinetically upon cocatalyst complexation, as the barrier roughly doubles in size for mono(imido) and somewhat less for bis(imido) species. Nonetheless, formation of tungstanacycle **3** appears as being most facile among all relevant steps, thus not likely affecting the catalytic behaviour.
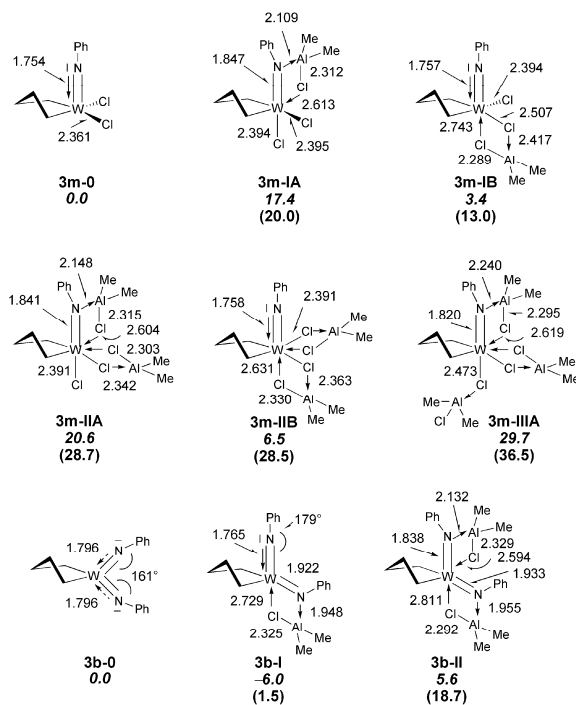

Figure 1: Most stable form of various modes of AlClMe$_2$ complexation onto **3m** (*top*) and **3b** (*below*). Bond lengths [Å] and relative stability [Δ*G* in kcal mol^{-1}] are given. Values in parentheses refer to the stability of adducts bearing a μ-Al–Me–W bridge.

4.1.3. Reactivity of **3** towards olefin substrate

The analysis of divergent paths starts by assessing the reactivity of **3** towards olefin substrate. The tungstanacycle imido intermediate has two potential sites for olefin attack, *viz.* the metallacycle fragment and the tungsten–imido linkage. Table 2 collects the energetics for **3** + C_2H_4 →**5** metallacycle growth and **3** + C_2H_4 →**6** [2 + 2] cycloaddition to commence from **3m** and **3b** having the $AlClMe_2$ activator complexed in various modes. As a general feature of both processes, olefin approach is indicated to not be associated with a substantial enthalpic barrier [29].

Ethylene insertion into the W^{VI}–C bond of the metallacycle fragment evolves through a transition-state (TS) structure comprising a quasi-planar four-membered *cis* arrangement of the W^{VI}–C bond and the coplanar oriented ethylene substrate. Considering the pathways associated with **3m-IB** and **3b-II** precursors as representative examples, the type B chelate stays in its original form during the whole process, whilst accommodation of incoming substrate onto **3b-II** goes along with the partial rupture of one chelate, having the N_{imide}→Al interaction still intact, which becomes rebuilt in **5**.

The **3** + C_2H_4 →**6** olefin cycloaddition across the tungsten–imido linkage proceeds via a four-membered TS structure having the two reactive bonds arranged near-coplanar. Cycloaddition commencing from **3m-IB** involves a product-like TS structure exhibiting significantly elongated tungsten–imido and olefin double bonds together with a relatively short new N–C bond (1.62 Å). In contrast, TS[**3**–**6**]**m-IA** features a very weak N_{imide}→Al interaction, as olefin attack at the arylimido group reduces its aptitude for cocatalyst association. Unsurprisingly, we have not been able to locate the TS for other type A modes **IIA**, **IIIA**. Concerning bis(imido) species, azacycle formation does occur at an earlier stage via a reactant-like TS structure.

The alternative steps exhibit similar kinetics for a given pathway involving mono(imido) or bis(imido) compounds (Table 2). This suggests a comparable likelihood for **3** + C_2H_4 →**5** and **3** + C_2H_4 →**6** being traversed from a kinetics point of view. Noteworthy, $AlClMe_2$ association does not discriminate between these steps. However, thermodynamics appears as being the discriminating factor. The growth of the metallacycle fragment is in most cases exergonic, driven by a moderate thermodynamic force (Table 2). On the other hand, the azatungstanacycle **6** is thermodynamically highly unfavourable (Table 2), thereby suggesting that the reverse **6**→**3** + C_2H_4 step is significantly more facile than **3** + C_2H_4→**6** azacycle formation. This led us to conclude that for both **3m** and **3b** the W^{VI}–C bond is the preferential target for olefin attack.

Metallacycle growth has computed barriers of 35.0 and 23.2 kcal mol^{-1} for unbound species **3m-0** and **3b-0**, respectively (Table 2). Type B Lewis acid complexation at W–Cl bonds of **3m** (**IB**, **IIB**, *cf.* Fig. 1) leaves the energy profile almost unchanged, whilst type A chelation (**IA**, **IIA**, **IIIA**, *cf.* Fig. 1) provokes an increase of the barrier by 6–7 kcal mol^{-1} (Table 2). A similar behaviour is seen for **3b**. Ethylene insertion into **3b-I**, where the second unbound imido ligand acts as a regulating factor (see above), exhibits an energy profile that is almost degenerate to that for **3b-0**. The reduction of the donor ability of both imido groups upon $AlClMe_2$ complexation increases the insertion barrier by ~10 kcal mol^{-1} (**II**, Table 2). Overall, the computational analysis presented thus far has disclosed that the cocatalyst exerts a moderate effect onto the formation and growth of tungstanacycle **3**, this in contrast to its profound influence on metallacycle degradation (see below).

Table 2: Calculated free-energy profile ($\Delta G^{\ddagger}$ in kcal mol^{-1})^a for **3** + C_2H_4 → **5** metallacycle growth and **3** + C_2H_4 → **6** [2 + 2] cycloaddition occurring along alternative channels

association mode[b]	TS[3–5]	5	TS[3–6]	6
mono(imido) **3m**				
0	35.0	–4.1	36.2	27.0
IA	40.8	–2.1	44.2	38.2
IB	33.7	–4.5	34.1	30.4
IIA	42.3	6.0	–	–
IIB	34.7	–4.8	35.5	31.8
IIIA	40.9	6.3	–	–
bis(imido) **3b**				
0	23.2	–9.6	23.6	15.5
I	22.6	–9.5	24.7	16.7
II	33.4	–1.4	33.2	20.3

[a] Intrinsic energetics relative to the respective precursor species **3m**, **3b**. [b] See Fig.1.

4.1.4. Degradation of 3

Degradation of the five-membered tungstanacycle to furnish the dimer product can either proceed though the stepwise mechanism depicted in Scheme 1, or alternatively via concerted 1,3-H transfer. The energetics of the two examined mechanisms is summarised in Table 3. Previous computational studies of the selective ethylene trimerisation by group 4 [17b-d], 5 [17a] and 6 [30] metal catalysts have provided significant evidence for the stepwise mechanism being preferential for the rigid five-membered metallacycle, whilst degradation of conformationally more flexible metallacycles follows the concerted pathway.

Starting with the stepwise degradation of mono(imido) and bis(imido) tungstanacycles, exemplified again for pathways linked to **3m-IB** and **3b-II**, the former sees some seemingly facile rearrangements of the bridging $AlClMe_2$ moiety at earlier stages until the TS for βH-abstraction is reached, in order to accommodate the shifted hydrogen. Decay of the TS leads to **4m-IB** having the alkenyl double bond complexed at the tungsten centre. The isomer where the alkenyl moiety is η^1-coordinated to the metal by is alkenyl terminus, although entropically favourable, does not represent the starting point for reductive CH-elimination (RE) evolving through the minimum-energy TS. This process does benefit from the coordinative stabilisation of the TS by the alkenyl double bond. Whilst passing through the TS for β-H abstraction from **3b-II**, one of the Lewis acid chelates is partially cleaved, but re-associates again in **4b-II** bearing a η^1-alkenyl moiety. Ensuing reductive dimer release evolves through an early TS structure that occurs at a distance of 1.35 Å for CH bond formation.

The availability of a vacant tungsten acceptor orbital is the major electronic factor that determines the kinetics of β-H abstraction [12]. Suitable tungsten orbitals, however, are unavailable for unbound **3m-0** and also for type B adducts **3m-IB**, **3m-IIB**, hence giving rise to an almost uniform barrier of ~30 kcal mol^{-1} (Table 3). Type A $AlClMe_2$ complexation, although thermodynamically unfavourable (see above), alleviates the kinetic blockage by the strong imido donor, which leads to a significant acceleration ($\Delta G^\ddagger$ ~20 kcal mol^{-1} for **3m-IA**, **3m-IIA**, **3m-IIIA**, *cf*. Table 3). A similar situation is seen for bis(imido) species. The rather small change in activation energy for **3b-I** relative to unbound **3b-0** is understandable, again, from the regulating influence of the second net six-electron donor imido group. Saturation of the immediate proximity around the tungsten centre by cocatalyst complexation, which amplifies the electrophilicity of the tungsten centre, facilitates the reductive elimination for the mono(imido) compound [12a], as the barrier decreases regularly upon increasing the number of associated $AlClMe_2$ moieties (Table 3). On the other hand, the unconquerable barrier for unbound species bis(imido) compound ($\Delta G^\ddagger$ = 72.4 kcal mol^{-1}, Table 3) drops substantially after confining the imido's donor capacity by cocatalyst complexation.

In light of the rather demanding stepwise degradation of **3b**, it may be conceivable that the concerted 1,3-H transfer, although demonstrated to be far less accessible for the conformationally rigid five-membered metallacycle [17], is predominant here. The TS structure associated with **3b-II** features two nearly equidistant C^β–H and $C^{\alpha'}$–H bonds, thus indicating a synchronous hydrogen shift, with the two chelates remaining intact. The Lewis acid appears to influence the precursor and TS in a comparable fashion, hence giving rise to a barrier of ~40–45 kcal mol^{-1} for

3b-I and **3b-II** that is similar to what is calculated for **3b-0** (Table 3). Given the size of this barrier it seems rather unlikely that the concerted mechanism becomes preferential for the mono(imido) tungstanacycle.

In conclusion, the stepwise mechanism is operative for dimer generation via mono(imido) and bis(imido) compounds. The computational survey has unveiled that the Lewis acid acts profoundly in smoothing the energy profile.

Table 3: Calculated kinetic profile ($\Delta G^{\ddagger}$ in kcal mol^{-1})^{a} for degradation of **3m** and **3b**

association mode^{b}	TS$_{\beta H\text{-}ab}$	TS$_{RE}$	TS$_{\beta H\text{-}trf}$
mono(imido) **3m**			
0	31.4	42.4	-
IA	18.9	29.2	-
IB	27.6	26.3	-
IIA	20.7	18.1	-
IIB	30.7	17.9	-
IIIA	18.2	13.0	-
bis(imido) **3b**			
0	37.4	72.4	44.0
I	34.3	57.1	44.9
II	24.4	36.5	40.5

^{a} Intrinsic energetics relative to the respective precursor species **3m**, **3b**. ^{b} See Fig.1.

4.2. Comparison of alternative dimerisation channels

Having assessed to what extent the cocatalyst affects individual steps, we now compare the located most accessible paths of the alternative channels shown in Scheme 1. It takes the tungstana(VI)cyclopentane intermediate **3** as the reference point, this in light of the previous findings that the oxidative coupling is a facile and basically thermoneutral step (see above) [31]. Starting the analysis with unbound species **3m-0**, **3b-0**, DFT predicts an almost insurmountable barrier for its degradation ($\Delta G^{\ddagger}_{RE\text{-}CH}$ = 42.4 and 72.4 kcal mol^{-1}, respectively) in conjunction with a kinetically easier growth to furnish **5** ($\Delta G^{\ddagger}_{INS}$ = 35.0 and 23.2 kcal mol^{-1}, respectively). Accordingly, dimer formation is almost entirely prevented and larger oligomers should likely be formed instead. This contrasts sharply with observed dimerisation abilities [11], thereby demonstrating that effective catalysis necessitates the active participation of the cocatalyst in the productive cycle; this in addition to its presumed role, among others, as alkylating and/or anion abstracting agent in the process of generating of the active catalyst.

Moving now to the realistic scenario where the Lewis acid does participate, the located most accessible pathway for the mono(imido) catalyst compound evolves through species where AlClMe$_2$ bridges the tungsten−chlorine bond in a four-membered chelate (Fig. 2). The operative stepwise mechanism for tungstanacycle degradation exhibits a double-well profile with a sufficiently stable, transient intermediate **4**, which can be expected as being to some extent populated. It may thus seem likely that seemingly facile AlClMe$_2$ association/dissociation does occur at this stage of the process. The first β-H abstraction has the higher barrier, thereby determining the effective kinetics of dimer formation. Notably, one AlClMe$_2$ moiety does participate in this step (commencing from **3-IB**), whilst the consecutive reductive CH-elimination does benefit from two cocatalyst moieties (commencing from **4-IIB**). DFT predicts β-H abstraction as being turnover limiting having a barrier of 31.0 kcal mol^{-1}, whilst competing olefin insertion into the metallacycle fragment ($\Delta G^{\ddagger}$ = 35.0 kcal mol^{-1} for **3m-0** + C$_2$H$_4$→**5m-0**) and [2 + 2] cycloaddition with the arylimido functionality ($\Delta G^{\ddagger}$ = 36.2 kcal mol^{-1} for **3m-0** + C$_2$H$_4$→**6m-0**) are significantly less probable, thereby rendering these routes almost impossible to traverse. All these aspects consistently reflect observed activity and selectivity, hence aid in rationalising the catalyst's abilities.

Lewis acid association at both arylimido functionalities appeared as being most effective in smoothing the energetics of dimer formation for the bis(imido) compound (see above). Degradation of **3b-II** displays a similar double-well profile, but with reductive elimination is now kinetically more demanding (Fig. 2). The associated

substantial total barrier of 48.1 kcal mol^{-1} indicates that this is likely not a viable step at operating reaction conditions. Instead, olefin attack at the two reactive sites of **3b-I** is clearly preferred kinetically ($\Delta G^{\ddagger}$ = 22.6/24.7 kcal mol^{-1} for **3b-I** + C$_2$H$_4$→**5b-I/6b-I**), such that the dimer generating path stays closed throughout.

The present computational survey constitutes some evidence that a mono(imido) tungsten compound, having the Lewis acid associated in a chelating fashion across one or two tungsten–chlorine bonds, can trigger dimerisation. This type of specific catalyst-cocatalyst interaction appears as being pivotal for achieving effective catalysis. Bis(imido) tungsten compounds, on the other hand, are indicated to not be responsible for observed catalyst's abilities. This raises questions concerning the identity of the active species for the case when a 1:2 molar ratio of tungsten and aniline starting materials is used [11]. It could also be a mono(imido) species, which may imply the abstraction of one imido ligand induced by the Lewis acid [32]. However, this aspect is beyond the scope of the present study and will be subjected to forthcoming studies.
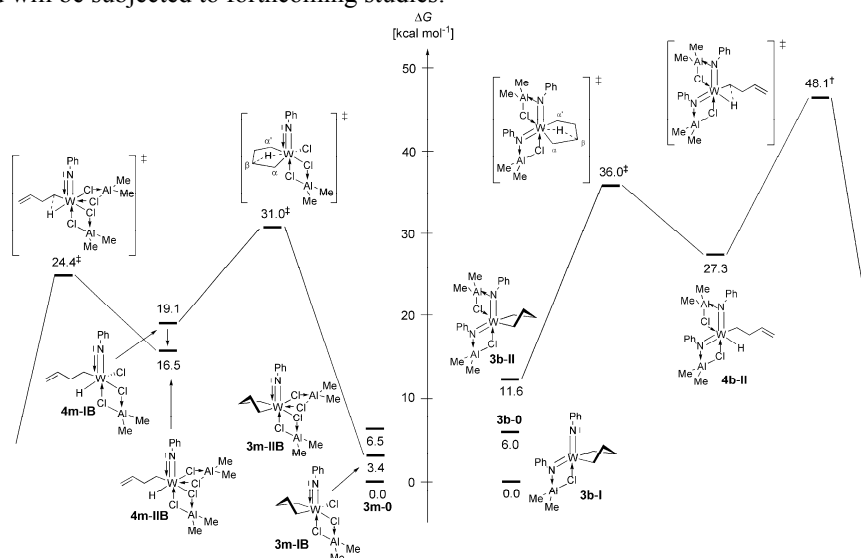

Figure 2: Calculated energy profile for dimer formation following the most accessible pathway of alternative reaction channels.

5. Concluding remarks

Tungsten imido compounds, when activated by a distinct amount of AlCl$_n$R$_m$ (m+n=3) cocatalyst, have been recently reported of being capable dimerising α-olefins [11]. However, little is known about the identity of the catalytically active species and the precise function of the Lewis acid component. Herein is reported a comprehensive computational survey of alternative dimerisation channels to engage mono(imido) and bis(imido) tungsten compounds on a realistic catalyst model and authentic reaction conditions. We performed an extensive DFT simulation of configurationally and conformationally different reaction pathways involving up to three AlClMe$_2$ moieties for all relevant steps of a plausible metallacycle mechanism. Furthermore, catalyst deactivation through formation of azatungstanacycle intermediates has been examined. The calculated reaction energy profile for unbound tungsten imido compounds is at odds with observed dimerisation abilities. The present study unveiled that effective catalysis necessitates the active participation of the Lewis acid component in the productive cycle, this in addition of its presumed role in the process of forming the active catalyst species. The AlClMe$_2$ component preferably forms four-membered chelates across tungsten–imido and tungsten–chlorine bonds featuring a μ-Al–Cl–W bridge. This does moderately affect the formation of the five-membered tungstanacycle key intermediate, but the Lewis acid acts profoundly in modulating the energetics of its degradation to furnish the dimer product. Of the alternative reaction channels, DFT predicts a smooth reaction profile for the most accessible path through mono(imido) tungsten compounds, with AlClMe$_2$ bridges across tungsten–chlorine bonds. This specific catalyst-cocatalyst association mode appears as being pivotal for achieving effective catalysis. The β-H abstraction is turnover determining with a barrier of 31.0 kcal mol^{-1} to furnish the dimer, whilst the route towards higher

oligomers is well separated and kinetically almost inaccessible. All these aspects are in consonance with observed activity and selectivity. The reaction channel through bis(imido) tungsten compounds displays a significantly more demanding energy profile, hence rendering it almost impossible to traverse. This implies that bis(imido) tungsten compounds are unlikely to play a role in the productive dimerisation course.

Acknowledgements

References and Notes

1 (a) W. Keim, Angew. Chem. Int. Ed. Engl. 29 (1990) 235; (b) J. Skupinska, Chem. Rev. 91 (1991) 613; (c) Y. Chauvin and H. Olivier, in Applied Homogeneous Catalysis with Organometallic Compounds, ed. B. Cornils and W. A. Herrmann, VCH, New York (1996) 258–268; (d) G.W. Parshall and S.D. Ittel, in Homogeneous Catalysis. The Applications and Chemistry of Catalysis by Soluble Transition Metal Complexes, Wiley, New York, 2nd edn. (1992) 72–85.

2 For recent reviews, see: (a) S.D. Ittel, L.K. Johnson and M. Brookhart, Chem. Rev. 100 (2000) 1169; (b) S. Mecking, Angew. Chem., Int. Ed. 40 (2001) 534; (c) V.C. Gibson and S.K. Spitzmesser, Chem. Rev. 103 (2003) 283.

3 (a) B.L. Small and A.J. Marcucci, Organometallics 20 (2001) 5738; (b) B.L. Small, Organometallics 22 (2003) 3178; (c) B.L. Small and R. Schmidt, Chem. Eur. J. 10 (2004) 1014.

4 R.D. Broene, M. Brookhart, W.M. Lamanna and A.F. Volpe, J. Am. Chem. Soc. 127 (2005) 17194.

5 K.P. Tellmann, V.C. Gibson, A.J.P. White and D.J. Williams, Organometallics 24 (2005) 280.

6 (a) B. Ellis, W. Keim and P. Wasserscheid, Chem. Commun. (1999) 337; (b) P. Wasserscheid and M. Eichmann, Catal. Today 66 (2001) 309.

7 (a) H.M. Menapace, N.A. Maly, J.L. Wang and L.G. Wideman, J. Org. Chem. 40 (1975) 2983. (b) H. Olivier and P. Laurent-Gerot, J. Mol. Cat. A: Chem. 148 (1999) 43.

8 A. Carter, S.A. Cohen, N.A. Cooley, A. Murphy, J. Scutt and D.F. Wass, Chem. Commun. 2002, 858.

9 (a) D.S. McGuiness, P. Wasserscheid, W. Keim, C. Hu, U.P. Englert, J.T. Dixon and C. Grove, Chem. Commun. 2003, 334; (b) D.S. McGuinness, P. Wasserscheid, W. Keim, D.H. Morgan, J.T. Dixon, A. Bollmann, H. Maumela, F.M. Hess and U. Englert, J. Am. Chem. Soc. 125 (2003) 5272.

10 A. Bollmann, K. Blann, J.T. Dixon, F.M. Hess, E. Killian, H. Maumela, D.S. McGuiness, D.H. Morgan, A. Neveling, S. Otto, M. Overett, A.M.Z. Slawin, P. Wasserscheid and S. Kuhlmann, J. Am. Chem. Soc. 126 (2004) 14712.

11 (a) M.J. Hanton and R.P. Tooze, WO 2005/089940 (Sasol Technology (UK) Ltd), 29 September 2005; (b) The {1 + Lewis acid} and {2 + Lewis acid} catalyst system are both highly selective to dimerisation (with %(higher oligomers+polymers) <1) and moderately active (N_t ~36 (1) and ~110 (2) (mol olefin)(mol W)$^{-1}$ h^{-1}, 60 °C); (c) M.J. Hanton, L. Daubney, T. Lebl, S. Polas, D.M. Smith, A. Willemse, Dalton Trans. 39 (2010) 7025.

12 (a) S. Tobisch, Organometallics 26 (2007) 6529; (b) S. Tobisch, Dalton Trans. (2008) 2120.

13 (a) R. Emmerich, O Heinemann, P.W. Jolly, C. Krüger and G.P.J. Verhovnik, Organometallics 16 (1997) 1511; (b) P.W. Jolly, Acc. Chem. Res. 29 (1996) 644.

14 (a) T. Agapie, S.J. Schofer, J.A. Labinger and J.E. Bercaw, J. Am. Chem. Soc. 126 (2004) 1304; (b) A.K. Tomov, J.J. Chirinos, D. J. Jones, R.J. Long and V.C. Gibson, J. Am. Chem. Soc. 127 (2005) 10166; (c) M.J. Overett, K. Blann, A. Bollmann, J.T. Dixon, D. Haasbroek, E. Killian, H. Maumela, D.S. McGuinness and D.H. Morgan, J. Am. Chem. Soc. 127 (2005) 10723.

15 (a) D.C. Bradley, M.B. Hursthouse, K.M.A. Malik, A.J. Nielson and R.L. Short, J. Chem. Soc., Dalton Trans. (1983) 2651; (b) D.C. Bradley, S.R. Hodge, J.D. Runnacles, M. Hughes, J. Mason and R.L. Richards, J. Chem. Soc., Dalton Trans. (1992) 1663; (c) S. Hayano and Y. Tsunogae, Macromolecules 39 (2006) 30.

16 (a) R.R. Schrock, R.T. DePue, J. Feldman, K.B. Yap, D.C. Yang, W.M. Davis, L. Park, M. DiMare, M. Schofiled, J. Anhaus, E. Walborsky, E. Evitt, C. Krüger and P. Betz; Organometallics 9 (1990) 2262. (b) H.H. Fox, K.B. Yap, J. Robbins, S. Cai and R.R. Schrock, Inorg. Chem. 31 (1992) 2287; (c) P.W. Dyer, V.C. Gibson and W. Clegg, J. Chem. Soc., Dalton Trans. (1995) 3313.

17 (a) Z.-X. Yu and K.N. Houk, Angew. Chem. Int. Ed. 42 (2003) 808; (b) A.N.J. Blok, P.H.M. Budzelaar, and A.W. Gal, Organometallics, 22 (2003) 2564; (c) T.J.M. de Bruin, L. Magna, P. Raybaud and H. Toulhoat, Organometallics 22 (2003) 3404; (d) S. Tobisch and T. Ziegler, Organometallics 22 (2003) 5392.

18 (a) R. Ahlrichs and coworkers TURBOMOLE V5.8: Quantum Chemistry Group, University of Karlsruhe, Germany (1988); (b) R. Ahlrichs, M. Bär, M. Häser, H. Horn and C. Kölmel, Chem. Phys. Lett. 162 (1989) 165; (c) O. Treutler and R. Ahlrichs, J. Chem. Phys. 102 (1995) 346.

19 (a) P.A.M. Dirac, Proc. Royal Soc. (London) A123 (1929) 714; (b) J.C. Slater, Phys. Rev. 81 (1951) 385; (c) J.P. Perdew and Y. Wang, Phys. Rev. B45 (1992) 13244; (d) J. Tao, J.P. Perdew, V.N. Staroverov and G.E. Scuseria, Phys. Rev. Lett. 91 (2003) 146401; (e) J.P. Perdew, J. Tao, V.N. Staroverov and G.E. Scuseria, J. Chem. Phys. 120 (2004) 6898.

20 D. Andrae, U. Häußermann, M. Dolg, H. Stoll and H. Preuß, Theor. Chim. Acta 77 (1990) 123.

21 A. Schäfer, C. Huber and R. Ahlrichs, J. Chem. Phys. 100 (1994) 5829.

22 (a) V.N. Staroverov, G.E. Scuseria, J. Tao and J.P. Perdew, J. Chem. Phys. 119 (2003) 12129; (b) Y. Zao and D.G. Truhlar, J. Chem. Theory Comput. 1 (2005) 415; (c) F. Furche and J.P. Perdew, J. Chem. Phys. 124 (2006) 044103.

23 D.A. McQuarrie, Statistical Thermodynamics, Harper & Row, New York (1973).

24 A. Klamt and G. Schüürmann, J. Chem. Soc. Perkin Trans. 2 (1993) 799.

25 S. Tobisch and T. Ziegler, J. Am. Chem. Soc. 126 (2004) 9059.

26 T.R. Cundari, Chem. Rev. 100 (2000) 807.

27 T.J. Crevier and J.M. Mayer, Angew. Chem. Int. Ed. 37 (1998) 1891.

28 P.D. Bolton, E. Clot, A.R. Cowley and P. Mountford, J. Am. Chem. Soc. 128 (2006) 15005.

29 Examination by a linear-transit approach gave no indication that this process has a significant enthalpy barrier.

30 W. Janse van Rensburg, C. Grove, J.P. Steynberg, K.B. Stark, J.J. Huyser and P.J. Steynberg, Organometallics 23 (2004) 1207.

31 An almost quantitative and sufficiently facile transformation of the starting materials into the bis(olefin) active catalyst species **2** is furthermore assumed. A practicable route has been previously suggested for bis(imido) tungsten compounds (see ref. 12b)

32 There is some presence for such processes, for instance in metathesis catalysis; see, for example: R.R Schrock and A.H. Hoveyda, Angew. Chem., Int. Ed. 42 (2003) 4592.